CHAPTER VI

MERCURY ARC PLASMA IN AN AXIAL MAGNETIC FIELD.

6.1. Introduction

Plasma parameters such as electron density and electron temperature undergo a change when the plasma is subjected to a magnetic field and in chapters III through V, it has been shown that when the magnetic field is transverse to the direction of flow of the discharge current, electron temperature increases and radial electron density decreases whereas if the magnetic field is longitudinal, the reverse effect takes place. The investigations have been carried out in molecular gases such as hydrogen, oxygen, nitrogen and air and in inert gas like helium. The parameters have been measured by Langmuir probe method and spectroscopic method. It is worthwhile to investigate whether the physical processes occuring in a glow discharge undergo any significant change when we pass from glow to arc region and in one of our previous investigations (Sen and Das, 1973) it has been established that in case of a mercury arc plasma carrying a current from 1 amp. to 2.5 amps., electron temperature increases in a transverse magnetic field and the results are in quantitative agreement with Beckman's theory (1948, modified by Sen et al,1971, 1972) specially

for small values of reduced magnetic field. The effect of a longitudinal magnetic field on a low pressure mercury arc has been investigated by various workers (Cummings and Tonks, 1941, Forrest and Franklin, 1966 and Vorobjeva, Zaharova and Kagan, 1971). The investigations were carried out in comparatively lower pressure region ($p \leq$ 0.2 torr) and there is shortage of data for comparatively high pressure large current plasma in longitudinal magnetic field.

In the present investigation the variation of current and voltage across a mercury arc plasma (admixed with air) as well as variation of electron temperature are studied in a longitudinal magnetic field. Most of the results reported for mercury arc plasma are with argon as background gas; in the present investigation air is the background gas, which enables us to study how the excitation, ionization and deionization processes are influenced by the presence of air.

In the case of molecular gases, the ionisation is mainly due to electron impact of the ground state molecule whereas in the case of mercury arc, ionisation is predominantly through inelastic electron impact with excited states like 6^3P_2 and with ground states and the phenomena of associative ionisation may also be present. Hence the physical processes occuring in a mercury arc plasma and how these processes are influenced by magnetic field have been taken into cosnideration in deducing the electron temperature and its variation in a magnetic field.

6.2. Experimental measurements and results

Experiments were performed on a d.c. mercury arc at low pressure burning in air. The discharge currents were 2.25 and 2.5 amps, while the dry air pressure was varied from 0.05 torr to 2 torr. Electron temperature T_e and T_{eB} without and with magnetic fields were determined by measuring the intensities of 5770 Å ($6^3D_2 \rightarrow 6^1P_1$) and 5790 Å (6^3D_1, $6^1D_1 \rightarrow 6^1P_1$) and taking their ratios. As the radiations differ by 20 Å they would have equal response to the photomultiplier tube (MIOFS29V λ) used. A vertical mercury arc tube of 10 cm. in length and 1 cm in radius, burning in dry air, and cooled externally was mounted in between the pole-pieces of an electro-magnet. A diffuse discharge filled the tube totally. An accurately calibrated constant deviation spectrograph was used to measure the wavelength of the spectral lines. The slit of the spectrograph was illuminated by condensing the light from the arc on the slit by a collimating lens. Each line was focussed on the cathode of the photomultiplier tube operated at 1425 volt. Detailed electronic arrangement for measuring the intensity of the spectral lines is given in Chapter II. The magnetic field (0 - 1100 gauss) was uniform inside the pole-pieces of the electromagnet. The pressure of air which was introduced through a needle valve, was measured by a McLeod gauge and the pressure of

mercury was determined from Handbook (1956) after noting the temperature of the inside wall by a mercury in glass thermometer (details in chapter II). Currents through the discharge was measured by an ammeter and the voltage across the tube was measured by a V.T.V.M. of internal resistance 35 MΩ. In the present investigation we have taken measurements with two types of arc discharges, (a) i = 2.25 am., p_{air} = 0.08 torr, p_{H_g} = 0.3032 torr, (b) i = 2.5 amp., p_{air} = 0.08 torr, and p_{H_g} = 0.3731 torr. The variation of current and voltage across the arc are noted for both type of discharges for a wide range of magnetic fields varying from 0 to 1100 gauss and a few representative data are shown in table 6.1. In fig. 6.1, discharge current, arc voltage and effective impedence of the arc have been plotted as a function of axial magnetic field B.

TABLE 6.1.

(Representative current/voltage variation with magnetic field).

Magnetic field in (Gauss)	i = 2.5 amp. p_{H_g} = 0.3731 torr, p_{air} = 0.08 torr.		i = 2.25 amp., p_{H_g} = 0.3032 torr, p_{air} = 0.08 torr.	
	Voltage across the arc(volts)	Current in amps.	Voltage across the arc(Volts)	Current in amps.
0	22	2.5	22	2.25
255	22.5	2.49	22.8	2.24
550	23.3	2.48	23.8	2.23
835	24.4	2.46	25.2	2.22
1050	25.5.	2.45	26.5	2.21

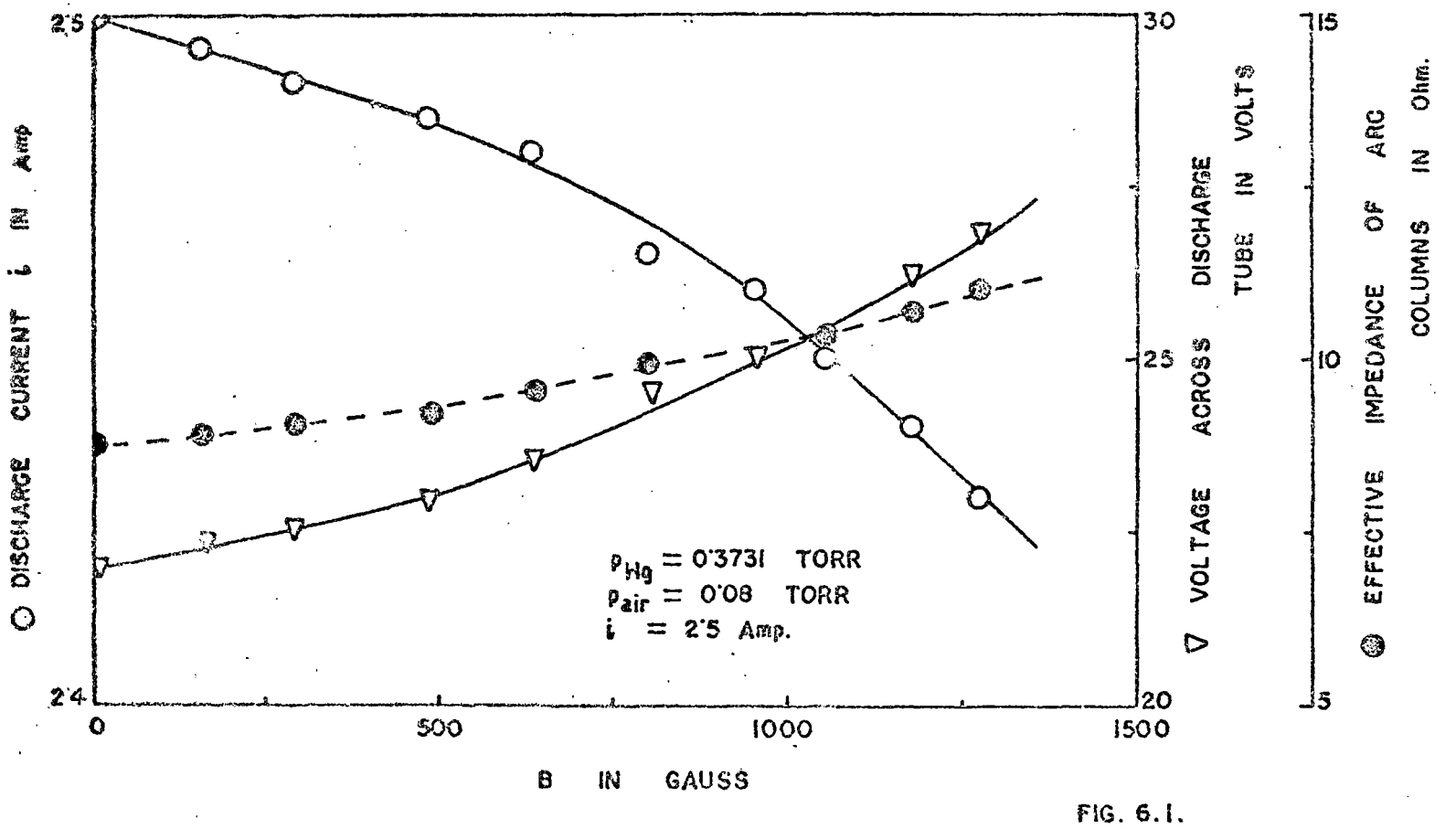

FIG. 6.1.

Fig. 6.1. Variations of arc current, voltage across the arc and effective impedance of arc column with a longitudinal magnetic field.

For measurement of electron temperature from the intensity of spectral lines, it has been shown by Griem (1964) that for LTE to be valid, the electron density n_e should be greater than 10^{16} cm^{-3}. Since cross section increases rapidly with principal quantum numbers whereas radiative decay rates decrease, the higher excited states may be in equilibrium with the continuum, which lead to idea of partial LTE, and the condition for partial LTE to be valid has been obtained by Griem (1964) as

$$n_e \geq 4.48 \times 10^8 \frac{1}{n^4} \left(\frac{kT_e}{E_H}\right)^{1/2} \sum_{i<k} A_{ki} \qquad (6.1)$$

where $\sum_{i<k} A_{ki}$ is the sum of all transition probabilities from the level k to all i's, $\sum A_{ki}$ values for levels $6^3D_{1,2}$ and 6^1D_2 are given by Mosberg and Wilkie (1978). E_H = 13.6 eV. and n is the effective quantum number of the state defined in chapter I. We thus find that $n_e > 10^{12}$ cm^{-3} for partial LTE to be valid for the levels and as our theoretical calculation shows that in the type of mercury arc discharge under investigation, $n_e \approx 10^{13}$ cm^{-3}, we can assume that partial LTE is valid in this case for the levels under consideration. Hence if we consider a transition $k \rightarrow i$ then the intensity of the line

$$I_{ki} = \frac{h\nu_{ki}}{4\pi} A_{ki} \frac{g_k}{g_i} n_1 \exp\left(-\frac{E_k}{kT_e}\right) \qquad (6.2)$$

and for a transition $j \rightarrow i$

$$I_{ji} = \frac{h l \nu_{ji}}{4\pi} A_{ji} \frac{g_j}{g_i} n_1 \exp\left(-\frac{E_j}{kT_e}\right) \qquad (6.3)$$

where ν and g's are the frequency of the transitions and statistical weights of the levels, A_{xi} is the transition probability for transition ($x \rightarrow i$), h is Planck constant and l is the length of plasma along the line of sight, From equations (6.2) and (6.3) it can be shown that

$$kT_e = \frac{E_j - E_k}{\ln\left[\frac{I_{ki}}{I_{ji}} \frac{A_{ji}}{A_{ki}} \frac{\lambda_{ki}}{\lambda_{ji}} \frac{g_j}{g_k}\right]} \qquad (6.4)$$

As the spectrograph used is unable to resolve the Zeeman spliting of the line in the magnetic field and the spectral intensity of the lines changes in the magnetic field it can be deduced from equations (6.2) and (6.3) that

$$\frac{1}{kT_{eB}} - \frac{1}{kT_e} = \frac{\ln\left[\frac{(I_{ki})_B}{I_{ki}} \Big/ \frac{(I_{ji})_B}{I_{ji}}\right]}{E_j - E_k} \qquad (6.5)$$

where $(I_{ki})_B$ and $(I_{ji})_B$ are the intensities of the lines in presence of magnetic field and T_{eB} is the electron temperature in magnetic field. The results for the measurement of intensities of the lines with and without

magnetic field and the corresponding electron temperature are shown in Tables 6.2 and 6.3. In fig. 6.2 variation of electron temperature with axial magnetic field for a mercury arc (i = 2.5 amp. p_{Hg} = 0.3731 torr and p_{air} = 0.08 torr) has been shown. In calculating electron temperature, $A_{\alpha i}$ g_{α} values have been taken from Mosberg and Wilkie (1978).

TABLE 6.2.

Variation of electron temperature with axial magnetic field for mercury arc (i = 2.5 amp., p_{Hg} = 0.3731 torr, p_{air} = 0.08 torr).

Magnetic field in (gauss)	$\frac{(I_{5790})_B}{I_{5790}} = x$	$\frac{(I_{5770})_B}{I_{5770}} = y$	$\ln(x/y)$	T_e in eV
0	1	1	0	0.422
255	1.02586	1.01852	7.1806×10^{-3}	0.313
550	1.08621	1.07407	1.1239×10^{-2}	0.282
835	1.14655	1.12963	1.4867×10^{-2}	0.256
1050	1.17241	1.15278	1.6887×10^{-2}	0.243

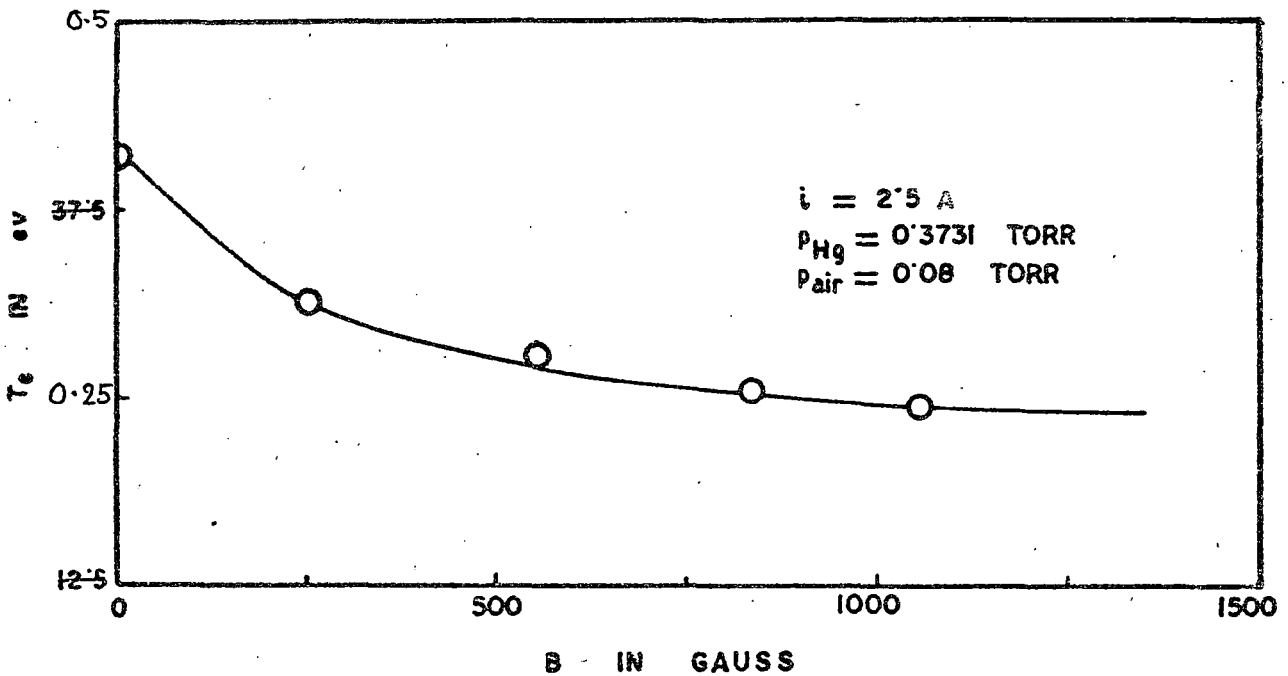

Fig. 6.2. Variation of electron temperature of a mercury arc discharge with longitudinal magnetic field.

TABLE 6.3

Variation of electron temperature with axial magnetic field for mercury arc (i = 2.25 amp., p_{Hg} = 0.3022 torr, p_{air} = 0.08 torr).

Magnetic field in (gauss)	$\frac{(I_{5790})_B}{I_{5790}} = x$	$\frac{(I_{5770})_B}{I_{5770}} = y$	$\ln(x/y)$	T_e in eV
0	1	1	0	0.412
255	1.02913	1.02	8.9072×10^{-3}	0.301
550	1.07282	1.06	1.2017×10^{-2}	0.276
835	1.13592	1.12	1.4116×10^{-2}	0.261
1050	1.19417	1.175	1.6187×10^{-2}	0.247

6.3. Discussion of Results

It is thus apparent from table 6.1 that when magnetic field is applied, the discharge current decreases and since the supply voltage to the arc is constant, the voltage across the discharge tube will increase.

To get the value of n_e the electron density we note that

$$i = \mu E e 2\pi \int_0^R n_r r dr \qquad (6.6)$$

where n_r is the radial electron density and μE

is the drift velocity of electrons for mercury and air mixture. For this type of discharge no data for μE is available so μE values for electrons in Hg. vapour is taken from the paper of Nakamura and Lucas (1978) and for the type of discharge where $p_{Hg} \gg p_{air}$ this result is likely to be more valid. Since the potential drop across the arc was observed to be nearly 22 - 24 volts with a cathode fall determined by Lamar and Compton (1931) as nearly 10 volts, the electric field E in the positive column of the discharge will be $E \gtrsim 1$ volt/cm and hence μE was taken to be 0.7×10^6 cm/sec. Now assuming Basselean distribution for electrons and putting $\frac{r}{R} = y$

$$i = e\mu E \, 2\pi R^2 \int_0^1 n_{eo} J_0 (2.405\, y)\, dy$$

or

$$i = e\mu E \, 2\pi \, n_{eo} \frac{R^2}{2.405} J_1 (2.405) \qquad (6.7)$$

where n_{eo} is the number density of electrons at the axis and R is the radius of the discharge tube. From the above equation we get the value of $\bar{n}_e$ the electron density averaged radially ($\bar{n}_e = 0.432\, n_{eo}$), when $i = 2.5$ amp., $\bar{n}_e = 1.645 \times 10^{13}$ cm^{-3} and for $i = 2$ amp, $\bar{n}_e = 5.687 \times 10^{12}$ cm^{-3}. This result

shows that for mercury arc discharge used here partial LTE is valid and equation (6.4) and (6.5) can be used for the measurement of T_e and T_{eB} respectively.

Further

$$i = e^2 E \frac{D_e}{kT_e} 2\pi \int_0^R r n_r dr \qquad (6.8)$$

and

$$i_B = e^2 E_B \frac{D_{eB}}{kT_{eB}} 2\pi \int_0^R r n_{rB} dr \qquad (6.9)$$

where D_e is the diffusion coefficient of electrons and the subscript B denote quantities in magnetic field. To get an expression for the electron density distribution, we have to consider the model of a mercury arc burning in air at low pressure.

The variation of voltage across the arc with axial magnetic field may be analysed in the following manner:

Let V_s = voltage generated by the source (a d.c. generator).

V_A = voltage across the arc

R = external resistance (ballast resistor) in the discharge circuit

and R_i = internal resistance of the source + control resistance in the source.

We can write,

$$V_s = i\ (R + R_i)\ V_A \qquad (6.10)$$

and similarly in a magnetic field

$$V_s = i_B\ (R + R_i)\ + V_{AB} \qquad (6.11)$$

From equations (6.10) and (6.11) it is evident that any increase in i would be associated with a decrease in V_A. From equations (6.10) and (6.11) we get

$$R + R_i = \frac{V_{AB} - V_A}{i - i_B} \qquad (6.12)$$

In fig. (6.3) $(V_{AB} - V_A)$ has been plotted against $(i - i_B)$ and the plot is a straight line in accordance to equation (6.12)

6.3.1. A model of a mercury arc burning in dry air

The discharge is axially homogeneous and cylindrically symmetric. The concentration of mercury ground state atoms (6^1S_0) is taken to be constant across the cross-section of the tube and is determined by the temperature of the wall. Only the mercury atoms are excited and ionised by electron impact. No line emission from air (i.e. N_2 or O_2) was observed. The concentration of the buffer gas which is dry air, is also uniform across the

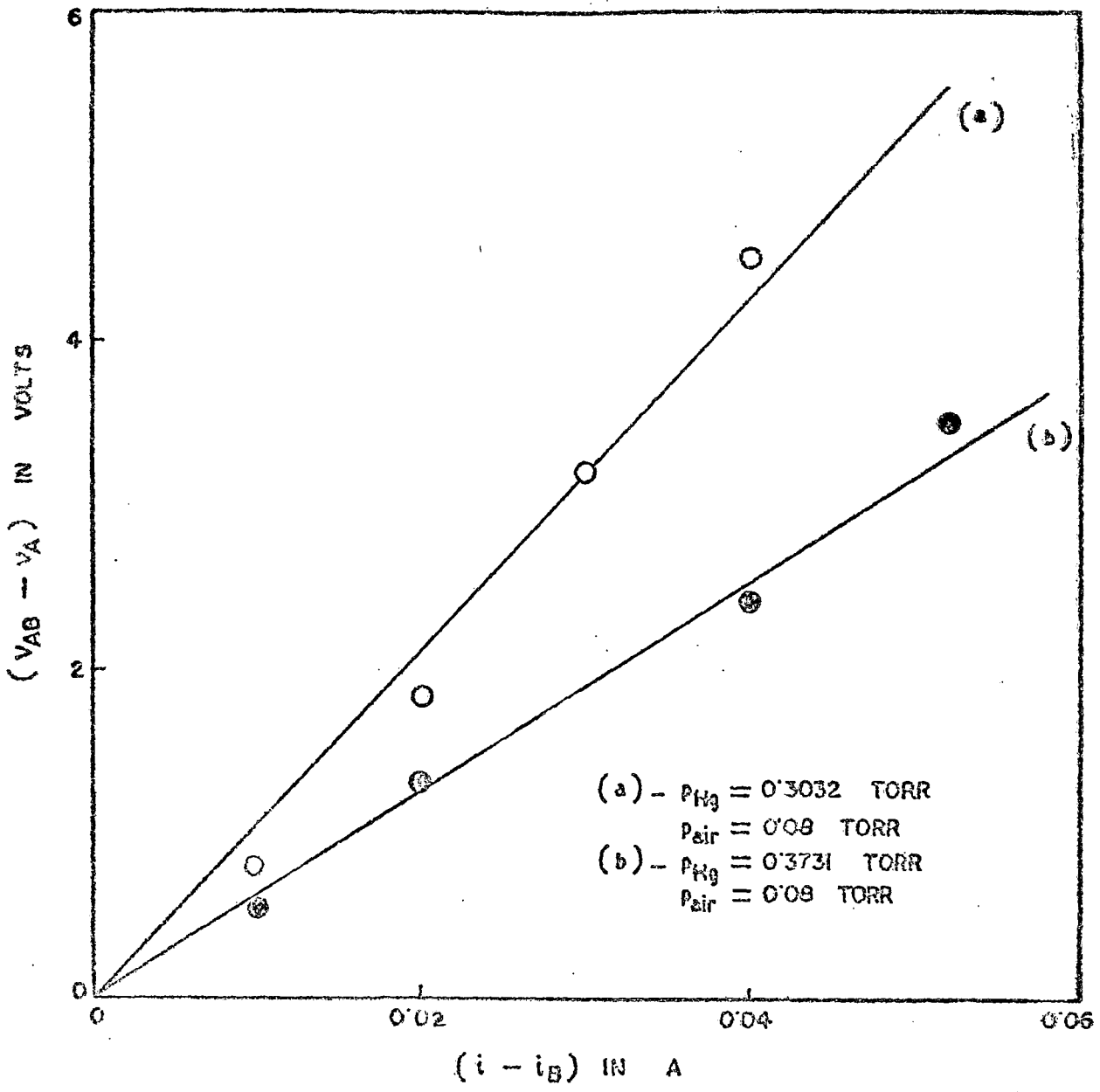

FIG. 6.3.

Fig. 6.3. Plot of $(V_{AB} - V_A)$ against $(i - i_B)$ for two types of mercury arcs discharges.

tube cross section and it plays a role in the ambipolar diffusion and mobilities of charged particles and in deactivating the excited mercury atoms. We disregard the depletion of mercury ground state atom density at the axis of the discharge tube which is generally observed in low gas temperature experiments. Assuming that (i) the principle excited species are 6^3P_2 6^3P_1 and 6^3P_0 with densities n_2 , n_1 and n_o respectively and cascading to these levels is not important in maintaining the densities and (ii) the diffusion losses can be accounted for ~~ad~~ by introducing a diffusion length; we can write the following equations for the excited species densities from the density balance equations of Forrest and Franklin (1969). For 6^3P_0 atoms:

$$-d_o n_o + E n_e n_g + W n_e n_1 + G n_1 n_g - (U+C+S) n_e n_o - H n_1 n_o - B n_o n_2 = 0 \qquad (6.13)$$

For 6^3P_2 atoms:

$$-d_o n_2 + F n_e n_g + J n_e n_1 - K n_2 n_g - (R+D+T) n_e n_2 - B n_o n_2 = 0 \qquad (6.14)$$

For 6^3P_1 atoms:

$$-d_o n_1 + L n_e n_g - \frac{n_1}{\tau} + M n_g n_p - (N+J+W) n_e n_1 - G n_1 n_g + T n_e n_2 + U n_o n_e - H n_o n_1 + K n_2 n_g = 0 \qquad (6.15)$$

$$-d_p n_1 - M n_g n_p + \frac{n_1}{\tau} = 0 \qquad (6.16)$$

where d_o is the loss coefficient for excited atoms through diffusion and n_g is the number density of mercury ground state atoms. d_p is the loss coefficient of resonance photons (2537 Å) and n_p is the number of photon particles per unit volume. In this way a five tier system for mercury is considered, the chief populating levels being ground state (6^1S_0), two metastable levels (6^3P_0, 6^3P_2), one resonance level (6^3P_1) and the mercury ions. The energy levels have been shown in fig. (6.4 a). The populations of ground state atoms are determined from inside wall temp. T_w of the discharge tube and populations of metastable and resonance levels can be determined from Forrest and Franklin's equations (6.13) to (6.16). The meaning of the terms in those equations has been entered into Table 4.4. As for example, the term $E n_e n_g$ means, rate (Sec.$^{-1}$) of the reaction

$$e + Hg\,(6^1S_0) \longrightarrow e + Hg\,(6^3P_0)$$

E is the rate coefficient given by

$$E = \langle v_e \sigma \rangle = \int_{v_0}^{\infty} v\,\sigma(v) f(v)\,dv$$

where σ is the cross section of the reaction, v_0 is the threshold value and $f(v)$ is velocity distribution function for electrons which is assumed

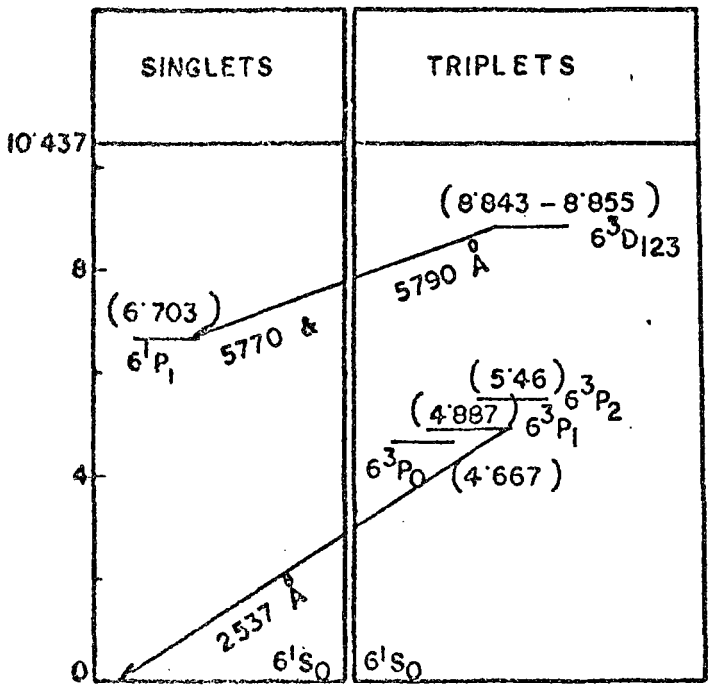

FIG. 6.4 a. ENERGY LEVEL DIAGRAM OF MERCURY (ENERGIES OF THE LEVELS SHOWN IN BRACKETS).

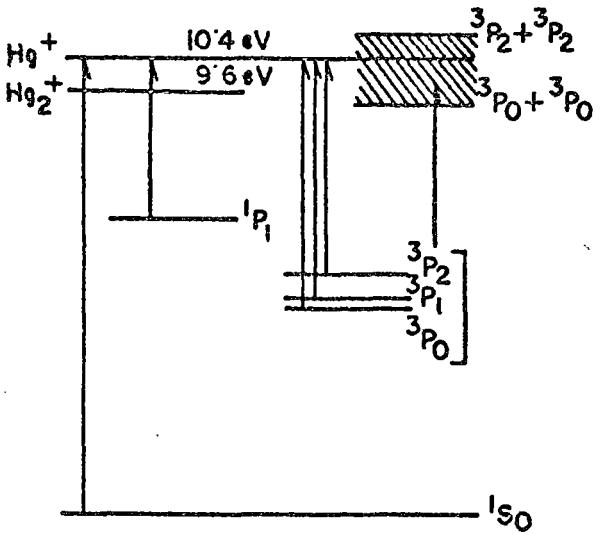

FIG. 6.4 b. IONISATION REACTION OF MERCURY ATOMS.

TABLE 6.4

Reactions considered in equation (6.13) to (6.16).

Term	Reaction	Calculated from equation no.
E	$e + Hg\ ^1So \longrightarrow e + Hg\ ^3P_o$	(6.23)
W	$e + Hg\ ^3P_1 \longrightarrow e + Hg\ ^3P_o$	(6.23)
G	$Hg\ ^3P_1 + Hg\ ^1S_o \longrightarrow Hg\ ^3P_o + Hg\ ^1So$	(6.24)
U	$e + Hg\ ^3P_o \longrightarrow Hg\ ^3P_1 + e$	(6.23)
C	$e + Hg\ ^3P_o \longrightarrow Hg^+ + e + e$	(6.25)
S	$e + Hg\ ^3P_o \rightarrow Hg\ ^1So + e$	(6.23)
H	$Hg\ ^3P_o + Hg\ ^3P_1 \rightarrow e + Hg_2^+$	(6.24)
B	$Hg\ ^3P_o + Hg\ ^3P_2 \rightarrow Hg^+ + e + Hg\ ^1So$	(6.24)
F	$e + Hg\ ^1So \rightarrow Hg\ ^3P_2 + e$	(6.23)
J	$e + Hg\ ^3P_1 \rightarrow Hg\ ^3P_2 + e$	(6.23)
K	$Hg\ ^3P_2 + Hg\ ^1So \rightarrow Hg\ ^3P_1 + Hg\ ^1So$	(6.24)
R	$e + Hg\ ^3P_2 \rightarrow Hg\ ^1So + e$	(6.23)
D	$e + Hg\ ^3P_2 \rightarrow Hg^+ + e + e$	(6.25)
T	$e + Hg\ ^3P_2 \rightarrow Hg\ ^3P_1 + e$	(6.23)
L	$e + Hg\ ^1So \rightarrow Hg^3P_1 + e$	(6.22)
N	$e + Hg\ ^3P_1 \longrightarrow Hg^+ + e + e$	(6.25)

Apart from these reactions other reactions considered in J.R. Forrest and R.N.Franklins' equations, are

$$Hg^3P_1 \longrightarrow Hg^1So + h\nu\ (2537\ \text{Å})$$

$$Hg\ ^1So + h\nu \rightarrow Hg^3P_1.$$

to be Maxwellian.

The presence of buffer gas like air will result into deactivation or quenching of excited species. Deactivation of excited Hg. atoms by N_2 and O_2 molecules have been studied thoroughly. It is assumed that energy differences are given to molecular gases as vibrational energies. Air constituents chiefly nitrogen and oxygen are found to be good deactivating agents. The chief deactivating processes are:

$$\text{I} \quad 6^3P_o + O_2 \longrightarrow 6^1S + O_2^*$$

$$\text{II} \quad 6^3P_1 + N_2 \longrightarrow 6^3P_o + N_2^*$$

$$\text{III} \quad 6^3P_1 + N_2 \longrightarrow 6^1S + N_2^*$$

$$\text{IV} \quad 6^3P_1 + O_2 \longrightarrow 6^1S + O_2^*$$

V deactivation of 6^3P_o atoms by Hg.

ground state atoms should be considered. The cross section of the processes are given in Massey, Burhop and Gilbody (1971),

$$\sigma_{\text{I}} = 0.31 \times 10^{16} \text{ cm}^2 \qquad \sigma_{\text{II}} = 1.3 \times 10^{-16} \text{ cm}^2$$

$$\sigma_{\text{III}} = 3 \times 10^{-16} \text{ cm}^2 \qquad \sigma_{\text{IV}} = 4.4 \times 10^{-16} \text{ cm}^2$$

$$\sigma_{\text{V}} = 23.9 \times 10^{-16} \text{ cm}^2$$

Including these processes in Forrest and Franklin's equations in (6.13) and (6.15)

$$-d_o n_o + E n_e n_g + W n_e n_1 + G n_1 n_g - (U+C+S) n_e n_o - H n_o n_1 - B n_o n_2 - Z n_g n_o - Y n_o n_{o_2} + X_1 n_1 n_{N_2} = 0 \qquad (6.17)$$

$$-d_o n_1 + L n_e n_g - \frac{n_1}{\tau} + M n_g n_p - (N+J+W) n_1 n_e - G n_1 n_g + T n_e n_2 + U n_o n_e - H n_o n_1 + K n_2 n_g - X n_1 n_{N_2} - V n_1 n_{o_2} = 0 \qquad (6.18)$$

where Z is related to process No. V

Y is related to process N0. I

X_1 is related to process No. II

X is related to process No. II + III

V is related to process No. IV

and n_{o_2} and n_{N_2} are the number densities of oxygen and nitrogen molecules.

To calculate the densities, we note that for 6^1S_o state atom densities are as follows:

$p_{Hg} = 0.3032$ torr, $n_g = 7.83 \times 10^{15}$ cm^{-3}

$p_{Hg} = 0.3771$ torr, $n_g = 1.3282 \times 10^{16}$ cm^{-3}

and evidently $n_g > n_2, n_1, n_o,$ or n_e

Equation (6.16) is the balance equation for resonance photons 2537 Å. The effective diffusion coefficient of resonance radiation at the wall has been shown by

Cayless (1963) to be

$$d_{pw} = \frac{g_j R^2}{8\tau} \qquad (6.19)$$

where τ = natural life time of 6^3P_1 atoms

$\approx$ 120 nsec (King and Adam (1974))

R = radius of the discharge tube = 0.75 cm.

g_j = Holstein's escape factor given, for cylindrical discharge tube, as

$$g_j = 1.60\left[k_0 R\left\{\pi \ln(k_0 R)\right\}^{1/2}\right]^{-1} \qquad (6.20)$$

$$k_0 = \frac{\lambda_1^3 n_g}{8\pi} \frac{g_k}{g_0} A_{k0} \left[\frac{M}{2\pi k T_g}\right]^{1/2} \qquad (6.21)$$

λ = 2537 Å, $g_k = 3$, $g_0 = 1$, $A_{k0} = 1/\tau$, M is the mass of mercury atom and kT_g is gas temperature (in eV), considered to be uniform across the cross section of the discharge tube and equal to the inner wall temperature kT_w. Putting these values in equation (6.16), value of ($-M n_p n_g + n_1/\tau$) may be calculated and this reduces the four particle balance equations to three.

To get the values of n_0 , n_1 and n_2 , as a first approximation we can neglect the terms $Jn_e n_1$ and $Bn_0 n_2$ in equation (6.14) as $n_g \gg n_2, n_1, n_0, n_e$ which leaves us with an equation containing and values of n_g and n_e are known. The values of different coefficients can be evaluated by assuming electron energy distribution to be Maxwellian and assuming the~~x~~ expression given by Sampson (1969) for optically allowed transition for electron impact ~~ionization~~ excitation as

$$\langle v_e \sigma \rangle = \pi a_0^2 \left(\frac{8kTe}{m\pi}\right)^{1/2} \left[4 f_{ij} \left(\frac{E_H}{E_0}\right)^2\right] \frac{2\pi}{\sqrt{3}} \frac{E_0}{kTe} P\left(\frac{E_0}{kTe}\right) \exp\left(-\frac{E_0}{kTe}\right) \qquad (6.22)$$

where $\pi a_0^2 = 8.797 \times 10^{-17}$ cm^2, E_0 is the ~~th~~ threshold energy of transition, f_{ij} the oscillator strength, For $(6^1So \rightarrow 6^3P_1)$ transition $f_{ij} = 0.0247$ (Skerbele and Lassttre, 1972). $P(E_0/kTe)$ is the Gaunt factor and values have been given by Sampson (1969). For optically forbidden transition we have taken the expression of Benson and Kulander (1972) utilising C.W.Allen's cross section,

$$\langle v_e \sigma \rangle = \frac{\pi a_0^2 4 E_H}{g_l E_0} \left[\frac{kTe}{2\pi m}\right]^{1/2} \exp(-E_0/kTe)\{1 - \exp(-E_H/kTe)\} \qquad (6.23)$$

here g_ℓ is the statistical weight of the state from which excitation is considered and E_H = 13.6 eV. For atom-atom/molecule reaction,

$$\langle v\sigma \rangle = \sigma \langle v \rangle = \sigma \left(\frac{8kT_g}{\pi \mu} \right)^{1/2} \qquad (6.24)$$

where σ is the effective cross section for the process considered and μ is the reduced mass of the colliding atoms and molecules.

Having determined the value of n_2 the equation for n_1 can be solved from equation (6.18) and putting this value of n_1 in equation (6.17), n_o can be obtained. Taking these values of n_o , n_1 and n_2 the equations are evaluated afresh by considering all the terms of the three equations. This procedure is repeated and the change in the values of n's is found to be small. Results of calculation of species densities are entered in Table 6.5.

To bring out the influence of buffer gas pressure calculations are given for p_{air} = 0.05 torr and p_{air} = 2 torr. In the calculations, diffusion coefficients of excited mercury atoms have been considered to be equal to that of ground state atom given in International critical Tables (1929). McDaniel (1964) has discussed that diffusion coefficient of excited atoms is rather small. However, calculations show that diffusion losses of excited atoms are negligible in comparison to collisional losses. This is inconformity with observations of Cayless (1963) and Polman et al (1972).

TABLE 6.5

Number densities of mercury atoms with varying conditions of discharge.

Condition of plasma			
	i	2.5 A	2A
	p_{air}	0.05 torr	2 torr
	p_{Hg}	0.3771 torr	0.222 torr
	T_e	0.5 eV.	0.5 eV.
Number densities in $cm^{-3} \times 10^{-10}$	n_{N_2}	1.424×10^5	5.667×10^6
	n_{O_2}	3.56×10^4	1.424×10^6
	n_g	1.328×10^6	7.83×10^5
	n_o	68.6	7.788
	n_1	19.13	1.423
	n_2	86.2	42.7
	n_e	1.64×10^3	5.687×10^2

Now let us look into the processes in these types of discharges. The chief ionization processes in a Hg. discharge are listed by Vriens, Keijser and Ligthart (1978) as

1. $Hg\ (6^1S_0) + e \longrightarrow Hg^+ + 2\ e$
2. $Hg\ (6^3P_0) + e \longrightarrow Hg^+ + 2\ e$
3. $Hg\ (6^3P_1) + e \longrightarrow Hg^+ + 2\ e$
4. $Hg\ (6^3P_2) + e \longrightarrow Hg^+ + 2\ e$
5. $Hg\ (6^3P_0) + Hg\ (6^3P_1) \longrightarrow Hg_2^+\ (6^2\Sigma^+) + e$
6. (a) $Hg\ (6^3P_1) + Hg\ (6^3P_2) \longrightarrow Hg^* + Hg\ (6^1S_0)$

   (b) $Hg^* + e \longrightarrow Hg^+ + 2\ e$

another process namely $Hg\ (6^3P_2) + Hg\ (6^3P_2) \longrightarrow$

$$Hg^+\ (6^2S_{1/2}) + Hg\ (6^1So) + e$$

is not considered by us as spin is not conserved in this process. The ionisation processes are shown in fig. 6.4(b). Electron impact ionisation rates from different levels K_1 to K_4 for processes 1 to 4 are given by Sampson (1969)

$$n_e n_i \langle v_e \sigma \rangle = 5{\cdot}465 \times 10^{-11} n_e n_i T_e^{1/2} \exp(-\chi_i / kT_e) \Gamma_i(T_e) \qquad (6.25)$$

$$i = g, 0, 1, 2$$

here T_e is the electron temperature in °K, χ_i is the ionisation energy of i^{th} level and $\Gamma_i = An/\chi_i^2$ where A = 200 for neutral atoms, n = number of electron per atom in the outer orbit. For process 5, the rate is

$$K_5 = n_o n_1 \langle v \sigma_5 \rangle = n_o n_1 \sigma_5 \langle v \rangle \qquad (6.26)$$

σ_5 is the effective cross section of associative ionisation. Tan and von-Engel (1968) have determined

$$\sigma_5 = 46 \times 10^{-15}\ cm.^2 \quad \text{and} \quad \langle v \rangle = \left(\frac{16\,kT_g}{\pi M}\right)^{1/2}$$

For process 6,

$$K_6 = n_1 n_2 \sigma_6 \langle v \rangle B_i \qquad (6.27)$$

σ_6 is estimated by Vriens et al (1978) to have a value of 10×10^{-15} cm^2, B_i is the Branching ratio and as calculated by the authors, B_i should be slightly less than unity i.e. all the atoms in the highly excited states populated by process 6 (a), are ionised by electron impact. Very few of them will make optically allowed transitions. We have neglected ionization from 6^1P_1 level, since the population density and natural life time of this level is small. With the help of equations (6.25), (6.26) and (6.27) and utilizing the values of n_e, n_g, n_0, n_1 and n_2 (table 6.5) the rate of ionization for the two types of discharges considered here has been calculated and are entered in Table 6.6.

TABLE 6.6

Ionisation rates with varying discharge condition.

Discharge conditions	Rate of ionization in Sec.$^{-1}$ x 10^{-11}					
	K_1	K_2	K_3	K_4	K_5	K_6
i = 2.5 amp. T_e = 0.5 eV. p_{air} = 0.05 torr p_{Hg} = 0.3731 torr	11.585	21.94	10.13	181.37	1700	466.4
i = 2 amp. T_e = 0.5 eV. p_{air} = 2 torr p_{Hg} = 0.222 torr	5.41	1.98	0.61	71.2	8.72	16.94

From the Table 6.6 it is evident that for a plasma where air pressure is comparatively small, ionization is chiefly through the process of associative ionisation and by electron impact ionisation of highly excited Hg. atoms whereas when p_{air} is comparatively large due to large quenching of 6^3P_0 levels ionisation will be primarily through the process of electron impact of 6^3P_2 atoms. So in type I plasma where p_{air} is small two types of ions Hg_2^+ and Hg^+ prevail inside the discharge tube. To calculate the normal distribution in a Hg discharge with two types of ions, we can utilize the equations of Golubovskii and Lyaguschenko (1977)

$$\left.\begin{aligned} \vec{j}_{i_1} &= -D_{i_1}\vec{\nabla}n_{i_1} + n_{i_1}\mu_{i_1}\vec{E}_r \\ \vec{j}_{i_2} &= -D_{i_2}\vec{\nabla}n_{i_2} + n_{i_2}\mu_{i_2}\vec{E}_r \\ \vec{j}_e &= -D_e\vec{\nabla}n_e - n_e\mu_e\vec{E}_r \end{aligned}\right\} \qquad (6.28)$$

j's are the current densities towards wall, n's are species densities, D and μ's are diffusion coefficients and mobilities and E_r is the radial electric field. Subscripts i_1 and i_2 denote atomic and molecular ions whereas subscript e denotes an electronic quantity.

Since $n_{i_1} + n_{i_2} = n_e$ and $j_{i_1} + j_{i_2} = j_e$ eliminating E_r from equation (6,28) and considering $\mu_{i_1} = \mu_{i_2}$ and hence $D_{a_1} = D_{a_2} = D_e\mu_i/\mu_e$

we get,

$$\left.\begin{aligned} \operatorname{div} \vec{j}_{i_1} &= -D_{a_1} \nabla\left(\frac{n_{i_1}}{n_e} \nabla n_e\right) = F_1 \\ \operatorname{div} \vec{j}_{i_2} &= -D_{a_2} \nabla\left(\frac{n_{i_2}}{n_e} \nabla n_e\right) = F_2 \\ F_1 + F_2 &= F_e \end{aligned}\right\} \qquad (6.29)$$

F_1, F_2 and F_e are the differences between the rates at which particles appear and disapper in the volume.

Kovar (1964) has shown that actually μ_{i_2}/μ_{i_1} = 1.875. It may be interesting to note that heavier ions are faster. The reason behind this is that atomic ions moving in their parent gas will have large charge exchange cross section and hence progress more slowly than the heavier molecular ions which do not suffer resonance charge exchange collisions. As the difference in values is not much and the presence of foreign gas will effectively reduce the charge exchange phenomena and obsecures the visions of Hg^+ ions for resonance to occur, the atomic and molecular ionic mobilities may be assumed equal.

Atomic ions will be produced mainly by (i) electron impact of highly excited states of Hg. atoms at rate $\nu_i n_e$ and these states are in thermal equilibrium with the electrons.

(ii) by electron impact dissociation of molecular ions with a rate $\vartheta n_{i_2} n_e$ and they will be lost mainly by

i) ambipolar diffusion to the wall,

ii) some of them will be converted to molecular ions in three body collisions at rate $K n_{i_1}$

Hence $$F_1 = \nu_i n_e + \omega n_{i_2} n_e - K n_{i_1} \qquad (6.30)$$

Molecular ions will be produced mainly by (i) the process of associative ionisation with rate g.

(ii) conversion of atomic ions at a rate $K n_{i_1}$ and they will disappear by

(i) ambipolar diffusion,

(ii) electron impact dissociation to atomic ions at a rate $\omega n_{i_2} n_e$

We have neglected dissociative recombination of molecular ions which is a comparatively slow process than the diffusion in an active discharge.

Hence, $$F_2 = g + K n_{i_1} - \omega n_{i_2} n_e \qquad (6.31)$$

In the above analysis it has been considered that the diffusion of charged particles towards the wall of the discharge tube is ambipolar in nature. For usual plasmas obtained by electric discharges, the diffusion can be considered ambipolar if $\lambda_D / \pi \Lambda \ll 0.01$ ie. if

$$n_e \gg 4.77 \times 10^4 \, (T_e / \Lambda^2) \quad cm^{-3} \qquad (6.32)$$

where λ_D is the Debye shielding length Λ is the diffusion length, T_e is temperature in °K. In the cylindrical geometry the lowest or fundamental diffusion length is given by

$$\frac{1}{\Lambda^2} = \left(\frac{2.4}{R}\right)^2 + \left(\frac{\pi}{L}\right)^2 \qquad (6.33)$$

Expression (6.32) has been confirmed experimentally by Gerber and Gerardo (1973). Calculations show that for R = 0.5cm., when $n_e \gg 5 \times 10^9$ the diffusion is ambipolar in nature.

Hence from equations (6.29), (6.30) and (6.31)

$$F_e = F_1 + F_2 = \nu_i n_e + g$$

$$= -D_{a_1} \nabla\left\{\frac{n_{i_1}}{n_e} \nabla n_e\right\} - D_{a_2} \nabla\left\{\frac{n_{i_2}}{n_e} \nabla n_e\right\}$$

as we have assumed $\mu_{i_1} = \mu_{i_2}$ and $D_{a_1} = D_{a_2} = D_a$

$$\nu_i n_e + g = -D_a\left[\nabla\left\{\frac{n_{i_1}}{n_e} \nabla n_e\right\} + \nabla\left\{\frac{n_{i_2}}{n_e} \nabla n_e\right\}\right]$$

or

$$\nu_i n_e + g = -D_a \nabla^2 n_e \qquad (6.33)$$

as $n_{i_1} + n_{i_2} = n_e$

we have neglected any distribution of excited state density across the tube cross section. In cylindrical co-ordinate system equation (6.33) reduces to

$$D_a \frac{1}{r}\frac{d}{dr}\left(r\frac{dn_r}{dr}\right) + g + \nu_i n_r = 0 \qquad (6.34)$$

Putting $r/R = y$ and $n_r/n_{eo} = N_r$ in equation (6.34) where n_{eo} is the number of density of electrons at the axis,

$$\frac{d^2N_r}{dy^2} + \frac{1}{y}\frac{dN_r}{dy} + \frac{R^2}{D_a}N_r\nu_i + \frac{gR^2}{D_a n_{eo}} = 0 \qquad (6.35)$$

Let us first consider the equation

$$\frac{d^2N_r}{dy^2} + \frac{1}{y}\frac{dN_r}{dy} + \alpha N_r = 0 \text{ where } \alpha = \frac{R^2\nu_i}{D_a}$$

Its solution is $y_1 = J_0(y\sqrt{\alpha})$ (6.36)

with conditions $N_r = y_1 = 1$ at $y = 0$ and we have

$$\frac{d^2y_1}{dy^2} + \frac{1}{y}\frac{dy_1}{dy} + \alpha y_1 = 0 \qquad (6.37)$$

Now multiplying (6.35) by y_1 and (6.37) by N_r and substracting we have,

$$\frac{d}{dy}\left[y\left(y_1\dot{N}_r - N_r\dot{y}_1\right)\right] = -\beta y y_1 \qquad (6.38)$$

where $\beta = \dfrac{g R^2}{n_{eo} D_a}$

On integration of (6.38) with conditions that at $y = 0$ both $\dot{y}_1$ and $\dot{N}_r = 0$, we have

$$y_1 \dot{N}_r - N_r \dot{y}_1 = -\frac{\beta}{\sqrt{\alpha}} J_1(y\sqrt{\alpha}) \tag{6.39}$$

Dividing (6.39) by y_1^2 we get,

$$d\left(\frac{N_r}{y_1}\right) = -\frac{\beta}{\alpha} \frac{d[J_o(y\sqrt{\alpha})]}{[J_o(y\sqrt{\alpha})]^2} \tag{6.40}$$

Integrating (6.40) with condition at $y = 1$, $N_r = 0$ we get,

$$N_r = \frac{g}{n_{eo} v_i} \left[\frac{J_o(y\sqrt{\alpha})}{J_o(\sqrt{\alpha})} - 1 \right] \tag{6.41}$$

Now at $y = 0$, $N_r = 1$, so

$$n_{eo} = \frac{g}{v_i J_o(\sqrt{\alpha})} \left[1 - J_o(\sqrt{\alpha})\right] \tag{6.42}$$

Hence, $n_r = N_r n_{eo}$

$$= \frac{n_{eo}}{1 - J_o\left(R\sqrt{\frac{v_i}{D_a}}\right)} \left\{ J_o\left(r\sqrt{\frac{v_i}{D_a}}\right) - J_o\left(R\sqrt{\frac{v_i}{D_a}}\right) \right\} \tag{6.43}$$

It is evident from equation (6.43) that the normal distribution in presence of magnetic field will be given by

$$n_{rB} = \frac{n_{eoB}}{1 - J_o\left(R\sqrt{\nu_{iB}/D_{aB}}\right)} \left\{ J_o\left(r\sqrt{\nu_{iB}/D_{aB}}\right) - J_o\left(R\sqrt{\nu_{iB}/D_{aB}}\right) \right\} \quad (6.44)$$

Cummings and Tonks (1941) from their experimental observation have predicted that the normal distribution for a mercury arc plasma is not affected by the presence of a longitudinal magnetic field, Hence, since the distribution is a function of ν_i / D_a, we can assume that $\nu_i / D_a = \nu_{iB} / D_{aB}$. Consequently from equations (6.8) and (6.9)

$$\frac{i}{i_B} = \frac{E}{E_B} \frac{D_e}{D_{eB}} \frac{T_{eB}}{T_e} \frac{n_{eo}}{n_{eoB}} \quad (6.45)$$

Bickerton and von-Engel (1956) have shown that if T_{eB} is not much different from T_e the fractional change of energy of an electron to its total energy also remains constant with magnetic field. This leads us to

$$E / E_B = T_e / T_{eB}$$

Hence

$$\frac{i}{i_B} = \frac{D_e}{D_{eB}} \frac{n_{eo}}{n_{eoB}} \quad (6.46)$$

Further if the change of electron temperature is small, then the rate of molecular ion formation due to associative ionisation will almost remain the same so that the

metastable population densities may be considered unaffected by the magnetic field. Since

$$\nu_i / D_a = \nu_{iB} / D_{aB}$$

we get from eqn. (6.42)

$$n_{eo} / n_{eoB} = \nu_{iB} / \nu_i \qquad (6.47)$$

Then from equation (6.46)

$$\frac{i}{i_B} = \frac{D_e}{D_{eB}} \frac{\nu_{iB}}{\nu_i} \qquad (6.48)$$

As we are considering electron impact ionization of highly excited states only and ν_i is given by Elton (1970) as,

$$\nu_i = n^* 9 \times 10^{-7} \left[\frac{\delta}{\chi_i} (kT_e)^{1/2} \right] \exp\left(-\chi_i / kT_e\right) \qquad (6.49)$$

where χ_i and n^* is the ionisation energy and number density of highly excited states. δ is a correction factor analogous to that used in the line broadening calculations for quadrupole interaction and other high order effects given by the larger of $(1 + 2K\, T_e / \chi_i)$ or 3. Considering δ and n^* to be invariant with magnetic field and since $\chi_i << kT_e$

$$\nu_{iB} / \nu_i = \sqrt{T_{eB} / T_e} \qquad (6.50)$$

Then,

$$\frac{i}{i_B} = \frac{D_e}{D_{eB}} \sqrt{\frac{T_{eB}}{T_e}} \qquad (6.51)$$

It is well known that when the frequency of ionization is much less than the frequency of momentum transfer,

$$D_{eB} = \frac{D_e}{1 + C_1 B^2 / p^2} \qquad (6.52)$$

where $C_1 = (e\lambda_{e1} / m v_r)^2$, λ_{e1} is the mean free path of electron at a pressure of 1 torr, p is the total pressure and v_r is the random velocity.

Hence from (6.51) and (6.52)

$$1 + C_1 \frac{B^2}{p^2} = \frac{i}{i_B} \sqrt{\frac{T_e}{T_{eB}}} = \frac{i}{i_B} \frac{n_{eoB}}{n_{eo}} \qquad (6.53)$$

A plot of $(i/i_B)(n_{eoB}/n_{eo})$ vs. $\frac{B^2}{p^2}$ (Figs. 6.5 and 6.6) will be straight line and the gradient determines the value of C_1 as entered in Table 6.7.

TABLE 6.7

Magnetic field in Gauss	$\frac{B^2}{p^2}$ x 10^{-6} Gauss^2/torr^2		$\sqrt{\frac{T_e}{T_{eB}}}$ (expt.)		$\frac{i}{i_B}$ (measured)		$\sqrt{\frac{T_e}{T_{eB}}} \times \frac{i}{i_B}$	
	X	Y	X	Y	X	Y	X	Y
0	0	0	1	1	1	1	1	1
250	0.44	0.3	1.169	1.138	1.002	1.0014	1.17	1.14
550	2.0	1.47	1.2218	1.2087	1.006	1.005	1.23	1.21
835	4.7	3.4	1.2564	1.2686	1.0117	1.011	1.27	1.28
1050	7.5	5.3	1.2915	1.302	1.0156	1.017	1.32	1.33

X Corresponds to i = 2.25 amp., p_{air} = 0.08 torr, p_{H_g} = 0.3032 torr, $C_1 = 0.3 \times 10^{-7}$

Y Corresponds to i = 2.5 amp., p_{air} = 0.08 torr, p_{H_g} = 0.3731 torr, $C_1 = 0.39 \times 10^{-7}$

Values of C_1 have been calculated from figs. 6.5 and 6.6.

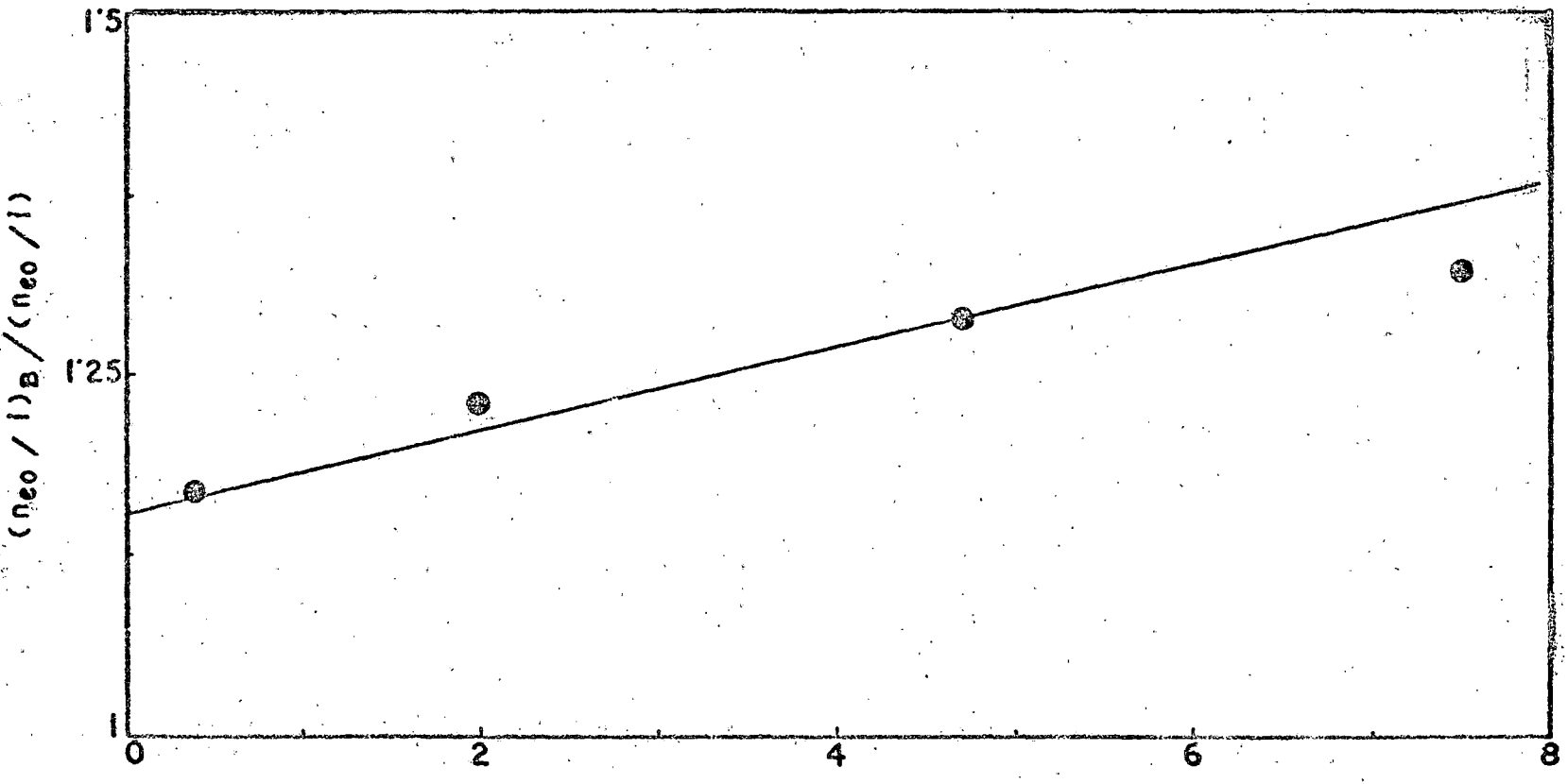

FIG. 6.5. Variation of $(n_{e0}/i)_B / (n_{e0}/i)$ with B^2/p^2 , i = 2.25 A.

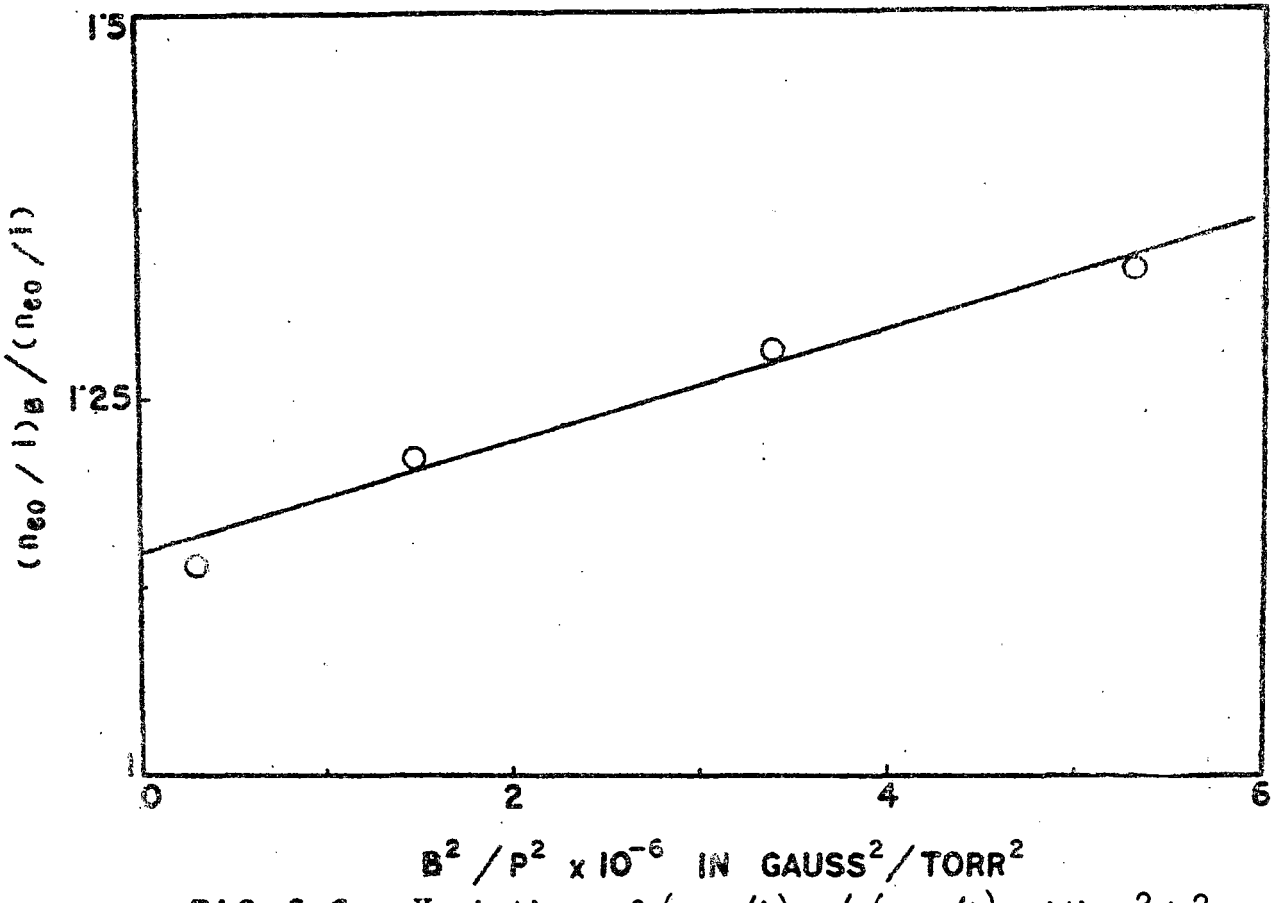

FIG. 6.6. Variation of $(n_{eO}/i)_B$ / (n_{eO}/i) with B^2/p^2, i = 2.5A.

6.4. Conclusions

Considering the physical processes involved in a mercury arc discharge where the buffer gas is air and the pressure is low, a model has been considered in which air plays the role of quenching gas and it has been found that in this type of discharge both atomic and molecular ions of mercury are present. Assuming the existence of both types of ions, we have obtained the distribution function and deduced an expression for T_e/T_{eB} and have found that within the range of B/p values used in the experiment, the experimental results are in quantitative agreement with the theoretical deduction.

That the electron temperature decreases in presence of an axial magnetic field in the case of mercury discharge, has also been shown by Franklin (1976). C_1 is evidently the square of the mobility of electrons in the mercury and air mixture at 1 torr. The value of mobility calculated from C_1 differs by an order of magnitude with that obtained experimentally by Nakamura and Lucas (1978). Further the results show that frequency of ionization changes with magnetic field as has been previously noted by Bickerton and von-Engel (1956).

It is also noted that

$$\frac{n_{eoB}}{n_{eo}} = \sqrt{\frac{T_e}{T_{eB}}}$$

and as experimentally we have found that $T_e > T_{eB}$, then $n_{eoB} > n_{eo}$ which was previously found to be true for molecular gases, as determined by Langmuir probe method in chapter III.

References:

1. Beckman, L. (1948) Proc. Phys. Soc. 61 515.
2. Benson, R.S. and Kulander, J.L. (1972) Solar Phys. 27 305.
3. Bickerton, R.J. and von-Engel, A. (1956), Proc. Phys. Soc. 76 468.
4. Cayless, M.A. (1963) Brit. J. Appl. Phys. 14 863.
5. Cummings, C.S. and Tonks, L. (1941) Phys. Rev. 59 514.
6. Elton, R.C. (1970) in Methods of experimental Physics 9 p. 149 (Academic Press, New York).
7. Forrest, J.R. and Franklin, R.N. (1966) Brit. J.Appl. Phys. 17 1569.
8. Forrest, J.R. and Franklin, R.N. (1969) J. Phys. B 2 Ser. 2 471.
9. Franklin, R.N. (1976) Plasma Phenomena in gas discharges (Oxford University Press).
10. Gerber, R.A. and Gerardo, J.B. (1973) Phys. Rev. A7 781.
11. Golubovskii, Y.B. and Lyaguschenko, R.I. (1977) Sov. Phys. Tech. Phys. 22 1073.
12. Griem, H.R. (1964) Plasma Spectroscopy (McGraw Hill, New York).
13. International Critical Tables for numerical data (1929) Vol.5, p. 62 (McGraw Hill, New York).
14. King, G.C. and Adam. A. (1974) J.Phys. B 7 1712.
15. Kovar, F.R. (1964) Phys. Rev. A133 681.
16. Lamar, E.S. & Compton, K.T.(1931) Phys.Rev.37 1069.

17. McDaniel, E.W. (1964) Collision phenomena in ionised gases p. 51 (John Wiley, New York).

18. Massey, H.S.W., Burhop, E.H.S. and Gilbody, H.B. (1971) Electron and ion impact phenomena, 2nd. Edn. Vol.3, p. 1693 (Oxford University Press).

19. Mosberg (Jr.) E.R. and Wilkie, M.D. (1978) J.Q.S.R.T. 19, 69.

20. Nakamura, Y. and Lucas, J. (1978) J. Phys. D. 11 325.

21. Polman, J. Nvander-Werf, J.E. and Drop, P.C. (1972) J.Phys. D. 5 266.

22. Sampson, D.H. (1969) Astrophys. J. 155 575.

23. Sen, S.N. and Das, R.P. (1973) Int.J.Electronics 34 527.

24. Sen, S.N., Das, R.P. and Gupta, R.N. (1972) J. Phys. D. 5 1260.

25. Sen, S.N. and Gupta, R.N. (1971) J. Phys. D. 4 510.

26. Skerbele, A. and Lassttre, E.N. (1972) J. Chem. Phys. 56 845.

27. Tan, K.L. and von-Engel, A. (1968) J. Phys. D. 1 258.

28. Vorobjeva, N.A., Zaharova, V.M. and Kagan, Yu, M. (1971) 9th.Int.Conf.on Phenomena in Ionised Gases p. 260.

29. Vriens, L., Keijser, R.A.J. and Ligthart, F.A.S. (1978) J. Appl.Phys. 49 3807.